Supporting Information

Graphene Template Induced Growth of Single-crystalline Gold Nanobelts with High Structural Tunability

Wenbo Xin, [a,*] Igor M. De Rosa, [a,b] Peiyi Ye, [a] Joe Severino, [a] Chao Li, [a] Xunqian Yin, [c] Mark S. Goorsky, [a] Larry Carlson [b] and Jenn-Ming Yang [a,*]

[a]*Department of Materials Science and Engineering, University of California, Los Angeles, 410 Westwood Plaza, Los Angeles, California 90095, USA*

[b]*Institute for Technology Advancement, University of California, Los Angeles, 410 Westwood Plaza, Los Angeles, California 90095, USA*

[c]*School of Materials Science and Engineering, Shandong University of Science and Technology, 579 Qianwangang Rd., Economic & Technological Development Zones, Qingdao, Shandong 26650, China*

* Corresponding Authors

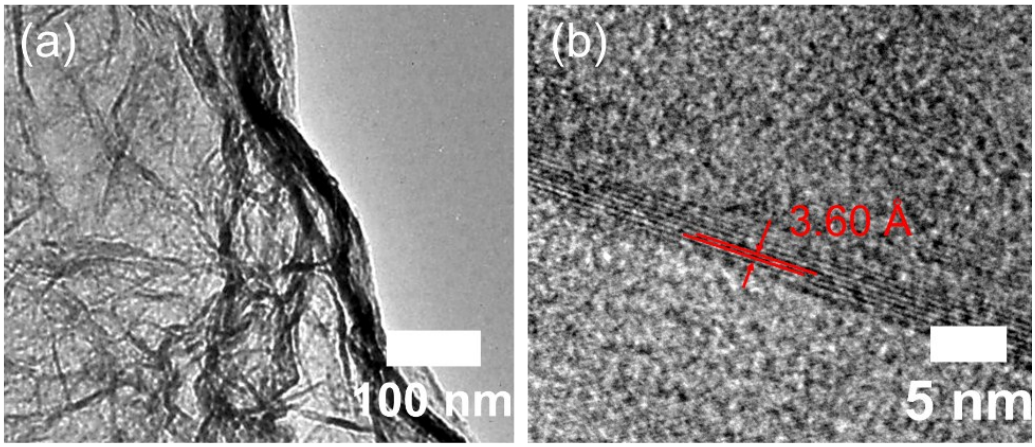

Figure S1. (a) Representative TEM image of *ml*G used in this work. (b) High resolution TEM image showing 11-layered graphene edge with the interspace of 3.60 Å.

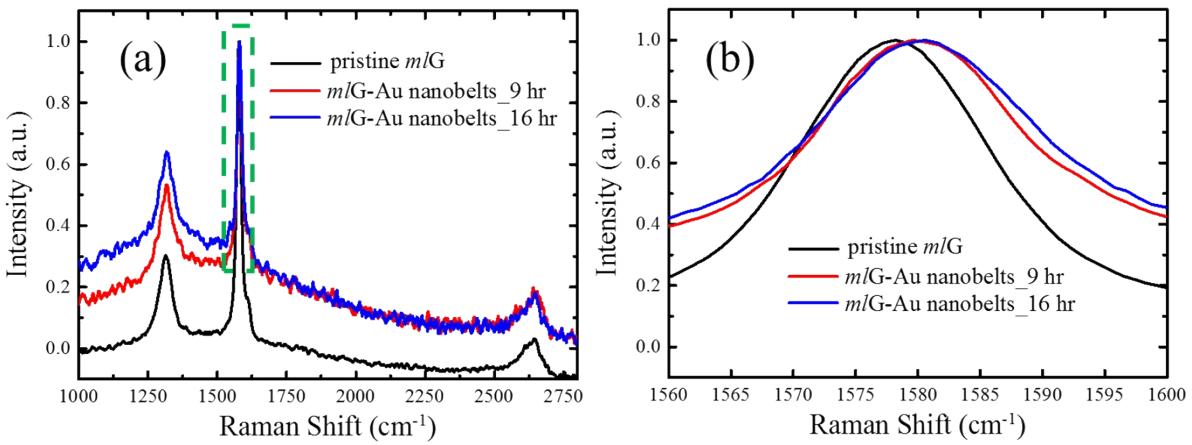

Figure S2 Raman spectroscopic characterization of *ml*G before and after reaction with gold precursor. (a) Normalized Raman spectra of pristine *ml*G, *ml*G-Au nanobelts at 9 hr and *ml*G-Au nanobelts at 16 hr in the range of 1000 cm^{-1} to 2800 cm^{-1}. (b) Raman spectra from 1560 cm^{-1} to 1600 cm^{-1} (the green dotted box in (a)) showing slight redshift of G peak with the reaction time.

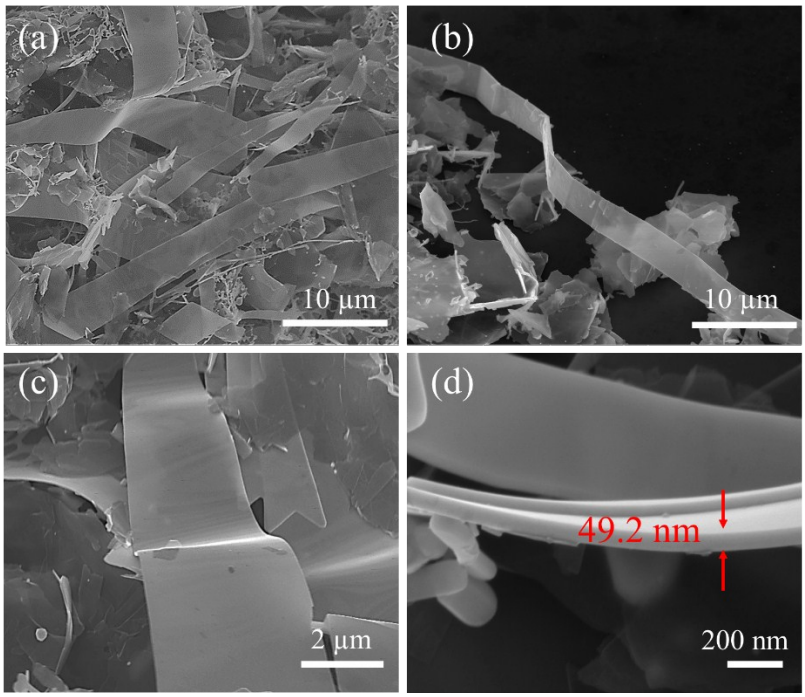

Figure S3. Morphologies of *ml*G-Au nanobelts. (a) Au nanobelts lying flat and parallel to the surface of multilayer graphene sheet. (b) An ultralong Au nanobelt isolated from the *ml*G template. (c) Au nanobelts fluctuating on graphene template. (d) Thickness of the nanobelts found to be sub-100 nm.

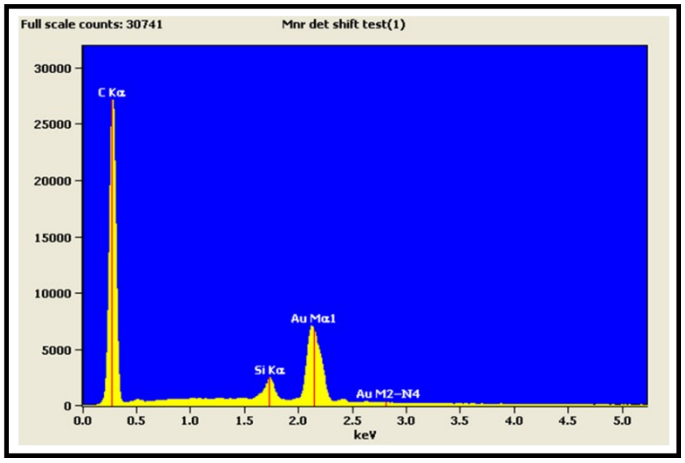

Figure S4. Elemental analysis of *ml*G-Au nanobelts. Only the elements of carbon, silicon and gold are recorded in the element spectrum. Note silicon signal originates from the substrate.

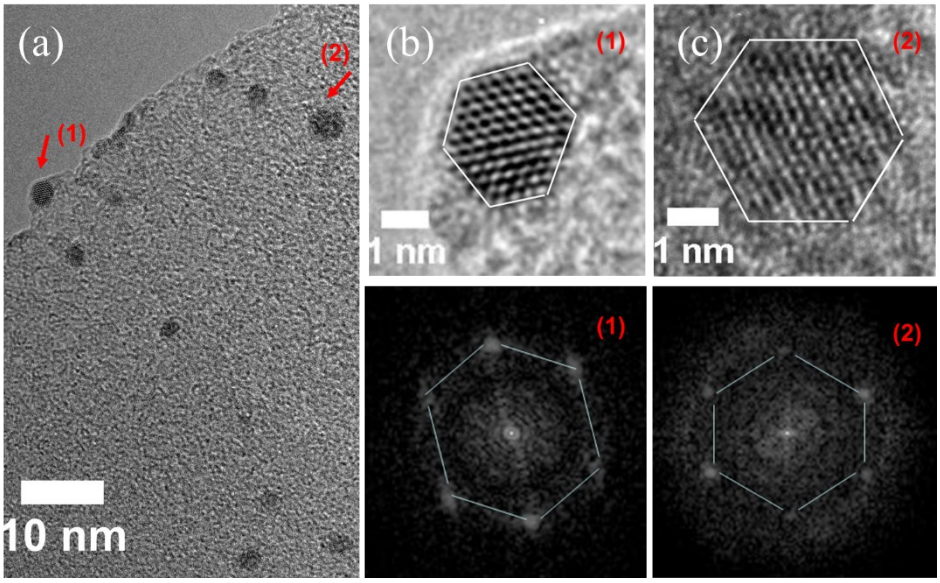

Figure S5. (a) TEM image of gold precursor reacting with graphene for 1hr. (b) and (c) Atomic structures and corresponding FFT patterns of two Au nanoplatelets in (a).

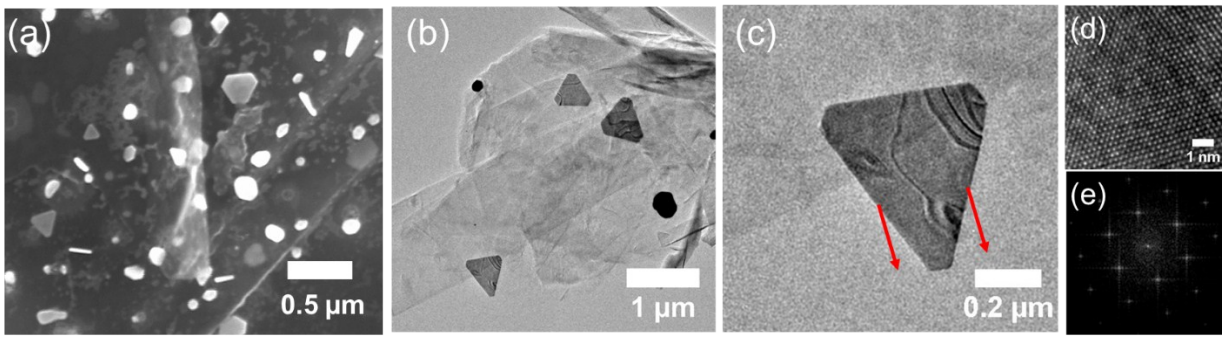

Figure S6. SEM image (a) and TEM image (b) of Au nanobelts grown on *ml*G template for 2 hr, forming Au nanoplates as the embryos of the nanobelts. (c) Selected Au nanoplates showing the favorable extending direction. (d) Atomic structure of selected area of (c). (e)The corresponding FFT of (d).

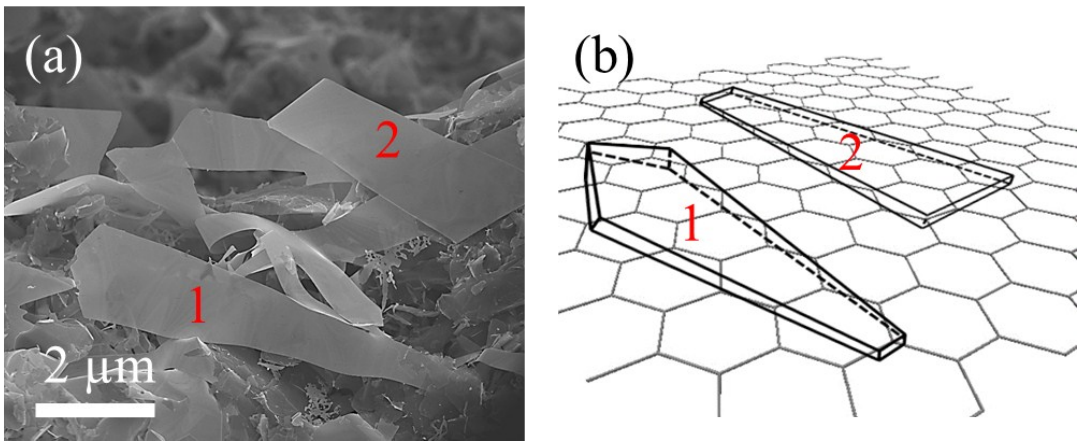

Figure S7. (a) Au nanobelts with two representative shapes. (b) Schematic image of two typical Au nanobelts: triangular and straight end.

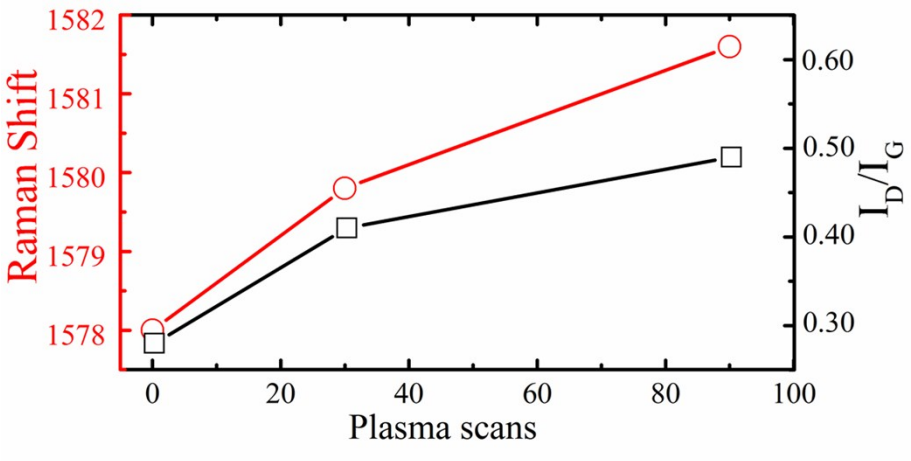

Figure S8. Raman shift of G peak and the modification of I_D/I_G of *ml*G with the number of plasma scans.

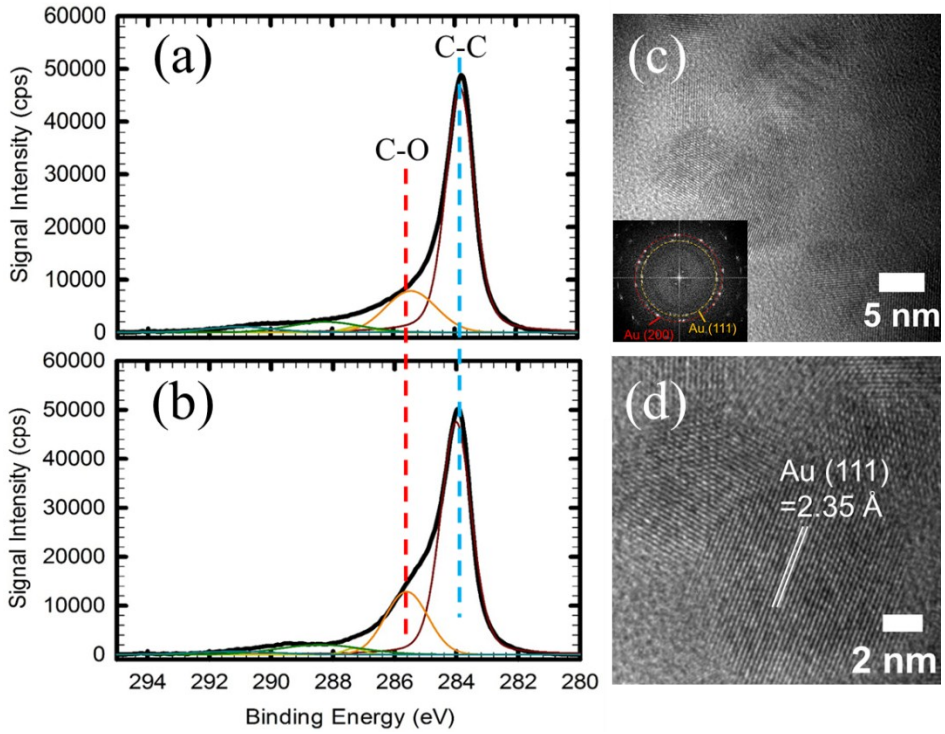

Figure S9. Quantification analysis of hydrophilic functional groups on *ml*G before (a) and after (b) oxygen plasma treatment (30 scans) using X-ray photoelectron spectroscopy. (c) A selected area of Au clusters nucleated on plasma oxidized *ml*G (30 scans) at 1 hr and ambient temperature. Inset is the corresponding FFT of the entire area. (d) Atomic structure of Au clusters selected in (c).

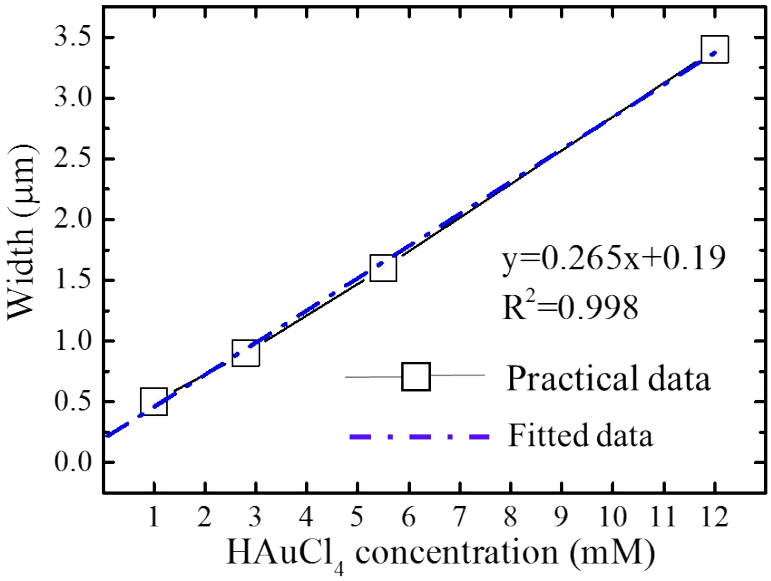

Figure S10. The relation between width of Au nanobelts and gold precursor concentrations.

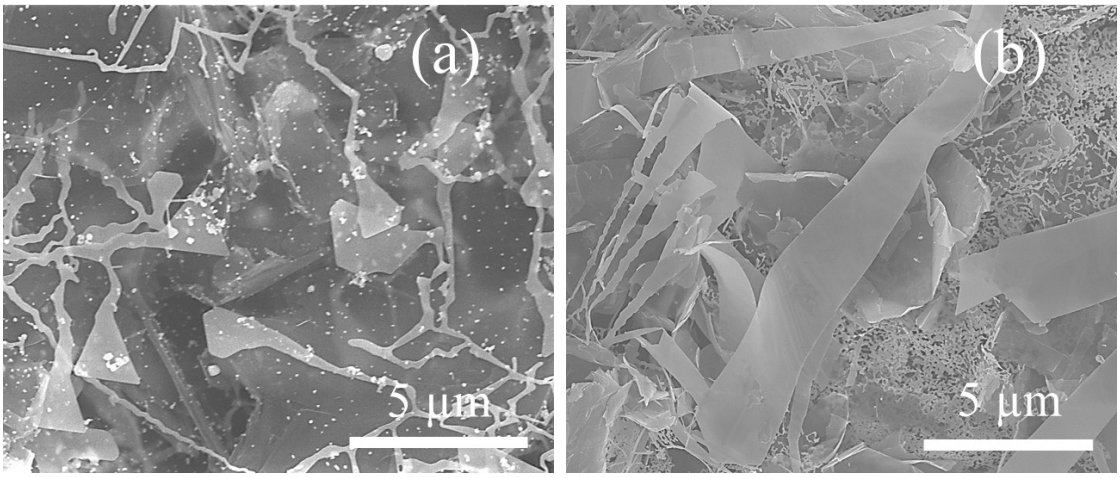

Figure S11. Au nanobelts synthesized on *ml*G by using12.0 mM $HAuCl_4$ at the time of (a) 4 hr and (b) 16 hr.